System identification methods on Alstom ECO 100 wind turbine

Iciar Font Balaguer
Alstom Wind
Roc Boronat nº 78, 08005
Barcelona, Spain
Iciar.font@power.alstom.
com

Stoyan Kanev
ECN Wind Energy
P.O. Box 1, 1175LE
Petten, the Netherlands
kanev@ecn.nl;

Dimitri Tcherniak
Bruel&Kjaer Sound and
Vibration Measurements
DK-2850 Naerum,
Denmark
dtcherniak@bkvs.com

Michele Rossetti
Alstom Wind
Roc Boronat nº 78, 08005
Barcelona, Spain
michele.rossetti@power.a
lstom.com;

Abstract

Traditionally, the design of control algorithms for wind turbines is performed based on (linearized) models of the wind turbine dynamics. Control performance is strongly dependent on the accuracy of these models and for this reason validation of the dynamics is essential for achieving optimal control. The aim of this work is to identify, at different wind speeds, the dynamic model of a wind turbine in operation by means of two different system identification techniques. This work has been partly performed within the SenternNovem long-term research project "SusCon: a new approach to control wind turbines" (EOSLT02013) and partly within the InVent project-ACC1Ó (CIDEM | COPCA).

Keywords: System Identification, wind turbine.

1 Introduction

Two different system identification methods have been applied on a wind turbine so to extract modal information at different operational conditions: Experimental modal analysis, where input/output signals are measured, and Operational modal analysis, where only output signals are measured.

On the Experimental modal analysis, the application of band-limited pseudo-random binary excitation signals (PRBS) have been carefully designed to avoid the induction of undesired significant loads on the tower and rotor, taking also into account the constraints of the actuators. When using Operational modal analysis, no forced excitation is needed and only the (unmeasured) ambient excitation from the wind is used. However, an elevate number of sensors must be used to recollect the vibrational responses since the modal parameters are dependent on the modal shape.

2 Theoretical background

2.1 Experimental Modal Analysis

Experimental modeling is an orthogonal approach to "first principles" physical modeling, where the phenomena observed in reality are modeled by using measured data from the operational wind turbine. To this end, system identification techniques are used to fit the parameters of a suitable mathematical model to the measured data as good as possible.

For wind turbine applications, experimental modeling has only received limited attention in the literature. The application of "exciter methods", where rather unrealistic direct and measurable excitation on several points on the blades is assumed, has been investigated in [1]. Recently, research on modal analysis has been performed within the framework of the European research project "STABCON" - Stability and control of large wind turbines", where both simulation studies and experimental results have been reported [2, 3]. The simulation studies are based on blade excitations that are difficult to realize in practice. More realistic excitation signals were investigated at Risø National Laboratory, where the use of the blade pitch and generator torque to excite the first two tower bending modes by harmonic signals and measurement of the decaying response proved to be unsuitable for

accurate estimation of the damping [3]. The identification of open-loop drive train dynamics from closed-loop experimental measurements on a fixed-pitch variable speed wind turbine for the purposes of control design algorithms is reported in [4].

Because the experimental modeling is based on data collected from a wind turbine during operation, i.e. with the controller in operation, closed-loop system identification must be applied. In this work, a detailed study is performed on the application of the following closed-loop identification (CLID) approaches to wind turbine model identification:

Direct method [5],

Indirect method [5],

Joint Input/output method [5],

Closed-loop instrumental variable method [6],

Tailor made instrumental variable method [7],

Closed-loop N4SID subspace identification [8],

Parsimonious subspace identification method (PARSIM) [9],

Subspace identification based on output predictions (SSARX) [10].

Initial studies using simulation data from both linear and nonlinear aeroelastic simulations have indicated that the methods Direct, SSARX and PARSIM are the most potential ones for wind turbine applications, with the Direct method often outperforming the other methods. For that reason, and for the sake of space limitation, only the Direct method is summarized in Section 2.1.2.

In order to identify accurate (unbiased) input-output models using the above-mentioned system identification methods, it is necessary that the inputs are additionally excited by signals that are uncorrelated with the wind. How this can be achieved without introducing unacceptable additional loads will be discussed in Section 2.1.1.

Finally, special attention has also been paid on data-driven model validation, for which purpose several techniques are developed and summarized in Section 2.1.3.
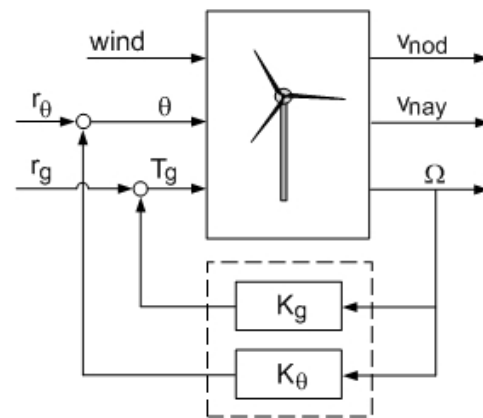
2.1.1. Excitation signal design

Figure 1. System identification setup

A possible system identification setup is depicted schematically on Figure 1. Typical inputs are the (collective) blade pitch angle θ and generator torque T_g setpoint, and outputs – generator speed Ω and tower fore-aft v_{nod} and sideward v_{nay} speed (or accelerations). The blocks K_g and K_θ in the feedback loops represent the torque and the pitch controllers, respectively, which are not required in the Direct identification methods, presented in Section 2.1.2. Time series of these typical inputs and outputs allow for the identification of the transfer functions from θ to v_{nod}, from T_g to Ω, and from T_g to v_{nay}, from which the tower fore-aft, tower side-to-side and drive train dynamics can be analyzed. The frequency region, in which the identified models will be accurate depend on the bandwidth of the excitation signals r_θ (on the blade pitch) and/or r_g (on the generator torque). When the frequency and damping of the first tower mode need to be identified, the bandwidth should at least include the (expected) first tower frequency. When the first drive-train mode is needed, the excitation bandwidth must at least include the first drive-train frequency. Hence, the proper choice of excitation signals is of paramount importance for achieving informative experiment under reasonable amount of excitation. In fact, there are two conflicting objectives, between which a trade-off should be made. On the one hand, a good excitation for system identification can be achieved by choosing a high energy excitation signal with wide flat spectrum. On the other hand, the system limitations (such as hardware limits, loads, etc.) necessitate the use of low-energy, narrow bandwidth excitation. The goal is to design

an excitation signal in such a way, that, (a), the signals remain within the hardware limits, (b) the additional loads are as small as possible, and (c), it still allows the identification of accurate models.

For the considered wind turbine, the excitation signals r_θ and r_g have been designed in such a way, that no unacceptable loads are induced, the excited pitch demand has acceptable speed and acceleration, and the electric power remains within acceptable limits. To this end,

> the pitch excitation signal r_θ is designed as a pseudo-random binary signal (PRBS) with amplitude of 0.5 degrees, filtered with a 31st order low-pass FIR filter with cutoff frequency of 1 Hz, and an elliptic bandstop filter with 20 dB reduction, 1 dB ripple, and stop-band of 30% around the expected first tower frequency (0.32 Hz). In this way the pitch excitation does not excite the region around the expected first tower frequency, as well as frequencies above 1 Hz.

> the generator torque excitation signal is also designed as PRBS signal, but uncorrelated with the one used for pitch excitation, and with an amplitude of 483.8 Nm (3% of the rated torque of 16.128 kNm), filtered with a 31st order lowpass FIR filter with cutoff frequency of 2 Hz, so that the excitation is concentrated in the frequency region up to 2 Hz.

Simulations made with an aerolastic code have revealed that these excitations introduce significant increment in loads.

2.1.2. Direct method for closed-loop identification

In the direct method [5], a so-called prediction error model identification is applied to the data, collected while the wind turbine operates in closed-loop. The starting point of the method is the selection of a suitable model structure. For wind turbine applications, a simple auto-regressive-with-exogenous-input (ARX) model proves to be sufficient. The ARX model has the following form

$$A(p).y(k) = B(p).u(k) + e(k) \qquad (1)$$

where $y(k) \in R^l$ is a generalized output vector, $u(k) \in R^m$ is the input vector,

$e(k) \in R^l$ is some unknown and immeasurable generalized disturbance signal representing the influence of the wind on the output measurements, k is the moment of time, and $A(P) \in R^{lxl}$ and $B(P) \in R^{lxm}$ are matrix polynomials dependent on the unknown parameter P:

$$A(P) = I + A_1 q^{-1} + A_2 q^{-2} + \cdots + A_{na} q^{-na},$$
$$B(P) = B_0 + B_1 q^{-1} + B_2 q^{-2} + \cdots + B_{nb} q^{-nb},$$
$$P = \left[A_1, \ldots, A_{na}, B_0, \ldots, B_{nb} \right]$$

Above, q^{-1} denotes the backward time shift operator, i.e. $q^{-1} y(k) = y(k-1)$.

The goal is to estimate the model parameters p given input/output data $\{u(k), y(k)\}_{k=1}^N$. This is achieved in the following way. Given the ARX model structure, the one step ahead predictor for the output vector is formed

$$\hat{y}(k) = P.\varphi(k),$$
$$\varphi(k) = vec([-y(k-1), \ldots - y(k-na), u(k), \ldots, u(k-nb)])$$

where vec(M) is the "vectorization" operator which stacks the columns of a matrix into one vector. This predictor model is used for constructing the prediction error

$$\varepsilon(k) = y(k) - \hat{y}(k) = y(k) - P\varphi(k) \qquad (2)$$

To estimate the unknown parameter matrix P, the following prediction error criterion is minimized with respect to P

$$V(P) = \frac{1}{N} \sum_{k=1}^N \frac{1}{2} \left\| \varepsilon(k) \right\|_2^2 \qquad (3)$$

An analytical expression can be obtained for the parameter matrix P that minimizes the prediction error criterion by using the fact that for given matrices of appropriate dimensions, the following expression holds

$$X.Y.Z = (Z^T \otimes X).vec(Y). \qquad (4)$$

Hence

$$\frac{\partial V(P)}{\partial vec(P)}$$
$$= \frac{\partial}{\partial vec(P)} \frac{1}{N} \sum_{k=1}^N \frac{1}{2} \left\| y(k) - (\varphi^T(k) \otimes I)vec(P) \right\|_2^2$$
$$= \frac{1}{N} \sum_{k=1}^N \frac{1}{2} (\varphi^T(k) \otimes I)^T \left(y(k) - (\varphi^T(k) \otimes I)vec(P) \right)$$

giving

$$vec(P) =$$

$$\left(\frac{1}{N}\sum_{k=1}^{N}(\varphi^{T}(k)\otimes I)^{T}(\varphi^{T}(k)\otimes I)\right)^{-1}\left(\frac{1}{N}\sum_{k=1}^{N}(\varphi^{T}(k)\otimes I)^{T}y(k)\right)$$

The identified ARX model is then parameterized by this optimal parameter matrix P. It can be theoretically shown that the identified model is unbiased under reasonable assumptions [5].

2.1.3. Modal parameters estimation

Once a model of the wind turbine is identified, there are different ways to extract modal parameters, such as the first tower and drive-train frequency and damping. One way to do that is by performing model reduction on the identified mode to reduce the model order, such that there is only one mode in a specified interval of interest where the frequency is expected to lie. For the considered wind turbine in this paper, this interval is chosen as [0.25,0.40] Hz for the tower, and [0.7,1] Hz for the drive train. The retained mode is the mode with the largest participation factor. The frequency and damping of this mode of the reduced system are then selected.

2.1.4. Model validation methods

Model validation is the process of deciding whether an identified model is reliable and useful for the purposes for which it has been created.

The following model validation methods have been used to check the accuracy of the identified model:

Variance-accounted-for (VAF): this is a model validation index often used with subspace identification methods. Given the measured output y(k) and the output predicted by the one step ahead predictor $\hat{y}(k)$, the VAF criterion is defied as

$$VAF(y,\hat{y}) = 1 - \frac{\sigma_{\varepsilon}}{\sigma_{u}} \qquad (5)$$

where σ_{y} is the variance of the signal y(k), and σ_{ε} - the variance of the prediction error ε. It is expressed in percentage. A VAF above the 95% is usually considered to represent a very accurate model.

Prediction error cost (PEC): this is the value of the prediction error cost function, defined above. The smaller the value, the better the model accuracy.

Auto-correlation index (R_{ix}^{ε}): when a consistent model estimate is made, the prediction error ε should be a white process, so that its auto-correlation function $R_{\varepsilon}(\tau)$ should be small for non-zero τ, where τ denotes the discrete time step. For a given confidence level α (e.g. $\alpha = 99\%$), a bound $R_{\varepsilon}^{bnd}(\alpha)$ can be derived such that for an accurate model the inequality $\left|R_{\varepsilon}(\tau)\right| \le R_{\varepsilon}^{bnd}(\alpha)$ should hold for all $\tau \ge 1$. The index R_{ix}^{ε} is then computed as the square sum of the distance between each value of the correlation function $R_{\varepsilon}(\tau)$ and the bound $R_{\varepsilon}^{bnd}(\alpha)$, where only the values outside the bound are used.

Cross-correlation index ($R_{ix}^{\varepsilon u}$): in the closed-loop situation the prediction error will be correlated with future values of the input, but should be uncorrelated with past inputs when the model is consistent. The cross-correlation function $R_{\varepsilon u}(\tau)$ should then be limited in absolute value for $\tau \ge 1$. The index $R_{ix}^{\varepsilon u}$ is computed similarly to R_{ix}^{ε}.

It is important to point out that the data set that is used for validating the models should be different from the data used for obtaining the model, as otherwise wrong conclusions could be drawn. When the data length is short, a rule of thumb is to use two thirds of the data for identification, and the remaining one third for validation.

2.2 Operational Modal Analysis

The ability to obtain modal characteristics of the big structures and particularly wind turbines played an important role in the establishment and further development of operational modal analysis (OMA). There are two significant advantages of OMA when one considers its application to wind turbine. First of all, OMA does not require the knowledge of the excitation forces; instead it applies the assumption that the forces are uncorrelated, distributed over

the entire structure and have flat broadband spectra. Secondly, since the tested structure is in its typical operational regime, all boundary conditions and the load levels are correctly reproduced: these conditions are very difficult to fulfill in the laboratory tests. This especially important for the aeroelastic damping estimation that varies with wind speed, wind direction, rotor speed and the blade pitch.

The following expression relates the (linear) response of the structure to the excitation forces:

$$\mathbf{x}(\omega) = \mathbf{H}(\omega)\mathbf{f}(\omega) , \qquad (6)$$

where $x(\omega)$ is the vector of the response spectra, $f(\omega)$ is the vector of the excitation spectra and $H(\omega)$ is the frequency response functions (FRF) matrix. From modal analysis theory, it is known that FRF matrix contains all necessary information to extract modal parameters. Applying simple algebra one can obtain

$$\mathbf{G}_{\mathbf{xx}}(\omega) = \mathbf{H}(\omega)\mathbf{G}_{\mathbf{ff}}(\omega)\mathbf{H}^{H}(\omega) , (7)$$

where $G_{xx}(\omega)$ is the response cross-spectra matrix and $G_{ff}(\omega)$ is excitation cross-spectra matrix. $(.)^{H}$ stands for matrix Hermitian (conjugate transpose).

Assuming the forces are uncorrelated, distributed over the structure and having flat broadband spectrum, its cross-spectrum matrix becomes $\mathbf{G}_{\mathbf{ff}}(\omega) \propto \mathbf{I}$ and

$$\mathbf{G}_{\mathbf{xx}}(\omega) \propto \mathbf{H}(\omega)\mathbf{H}^{H}(\omega) . \qquad (8)$$

This proves that, if the excitation assumptions fulfilled, the response cross-spectrum matrix contains the full information required to obtain (un-scaled) modal model of the system.

Excitation due to wind turbulence fulfills the abovementioned assumptions, which makes the application of OMA to *standstill* wind turbine a straightforward task. Paper [11] proves the feasibility of the method. However, the application of OMA to *operational* wind turbines is not simple. It is being considered in the next sections.

2.2.1. Violation of the Time invariance assumption

One of the fundamental assumptions behind any experimental modal analysis techniques is that the structure under test must not change during the test (so-called structure invariance). It is not the case for *operational* wind turbines: the rotation of the rotor must be somehow taken into account.

The effect of rotor rotation manifests itself in the equation of motion: the mass, stiffness and gyroscopic force matrices become time-dependent. Formulating and solving the eigenvalue problem for this case lead to time-dependent eigenvalues and eigenvectors which become meaningless as modal parameters. Fortunately, so-called *Coleman coordinate transformation* (also known as multi-blade coordinate transformation) allows one to eliminate time dependency of the system matrices, thus converting the original time-varying eigenvalue problem to a time-invariant one. The modal parameters: modal frequencies, damping and mode shapes are then obtained by solving the corresponding eigenvalue problem.

Study [12] extends this approach to experimental modal analysis. Forward Coleman transformation is applied to the data measured on the wind turbine blades, which is then combined with responses measured on the tower. The OMA methods are then applied to the transformed data, resulting in modal frequencies, damping and mode shapes. Backward Coleman transformation is finally employed for the mode shapes for their visualization.

2.2.2. Violation of the excitation assumptions

Analyzing interaction between wind turbulence and rotating blades [13], it is possible to show that the aerodynamic forces do not fulfill OMA assumptions: first of all the forces acting at different parts of the blades are correlated around fundamental frequency and its harmonics. Secondly the forces have periodic nature which manifests itself by peaks on force frequency spectra. The peaks are located at the fundamental frequency and its harmonics and have "thick tails" which narrows the regions where OMA assumptions are valid.

In [12] a careful experiment planning is suggested as a tool to avoid the frequency regions where OMA assumptions are not fulfilled.

3 Results

3.1 Experimental Modal Analysis Results

Time domain closed-loop system identification methods (CLID) are applied to both simulated data, used to verify loads and to check identification methodologies, and measurement data from an Ecotècnia 100 wind turbine using PRBS signals as defined in section 2.1.1. Figure 2 and 3 show the PRBS excitation signals added to the collective pitch and generator torque demand following the scheme presented in Figure 1.
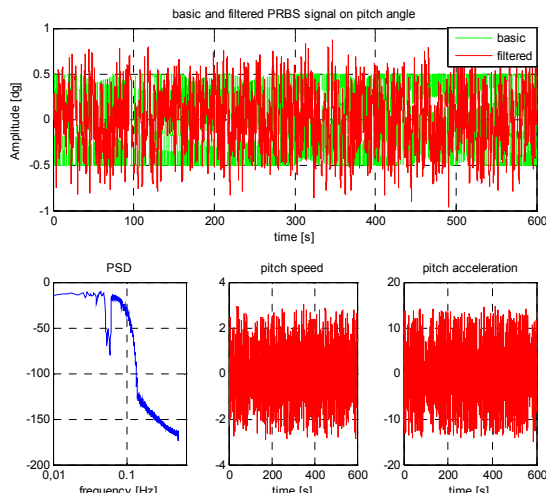

Figure 2.: PRBS excitation signal on collective pitch.

As explained in section 2, Closed-loop identification techniques are used to identify open loop models. Given the identified models, the corresponding frequency and damping of the first tower fore-aft and sidewards mode and the first drive train mode of the open-loop wind turbine can be computed at different wind speeds. Time and frequency validation methods are used to evaluate each method.

As first step, closed-loop identification techniques are applied to (excited) input/output data from aeroelastic simulations. Simulations show that no significant loads were induced on the turbine, the excited pitch demand had acceptable speed and acceleration, and
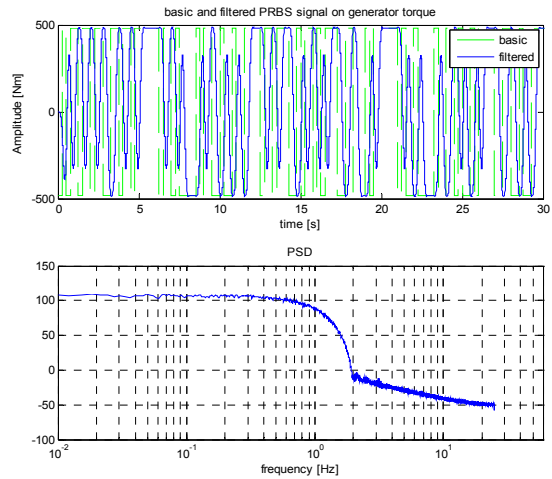

Figure 3: PRBS excitation signal on generator torque.

the electric power remained within acceptable limits.

As second step, studies on the closed-loop identification methods are carried out using simulation data. Since information about the controller and the exact excitation signals used ($r_θ$ and r_g from Figure 1) is not given, the Direct, SSARX and PARSIM demonstrate to be the most promising methods for wind turbine applications.

3.1.1 The measurement campaign

The same closed-loop identification techniques are applied using real (excited) input/output data collected from measurements on Alstom ECO 100 3MW wind turbine. The measurement campaign was performed at below rated wind speeds varying between 4 and 8m/s. The control inputs, collective pitch demand and generator torque demand, have been simultaneously excited with the PRBS signals s in order to make the identification of the transfer functions from these inputs to the outputs generator speed and tower top fore-aft and sidewards velocities possible. The input/output measurement data collected is summarized in the following table:

Generator speed Ω	rpm
Tower top fore-aft acceleration $\dot{v}_{fa}$	m/s^2
Tower top fore-aft acceleration $\dot{v}_{sd}$	m/s^2
Excited blade pitch angle demand θ	deg
Excited blade pitch angle demand T_g	Nm
Wind speed at nacelle V_{nac}	m/s

Table 1.: Signals stored from the real wind turbine

Experience shows that working with tower top velocities improves the quality of the identified models around the first tower modes. Hence, for the estimation of the tower modes, the outputs $\dot{v}_{fa}$ and $\dot{v}_{sd}$ are integrated to velocities v_{nod} and v_{nay}.

Four measurement time series are available, each taken during partial load operation. Due to the fact that each of these four measurements cases contains some irrelevant information from the identification point of view, they haven been concatenated as indicated in the following table.

Test case	Data length	Mean (Vnac)	Purpose
Test 1	1459s	4.5115m/s	ident.4.5m/s
Test 2	1130s	4.7783m/s	Valid.4.5m/s
Test 3	1651s	6.1169m/s	Ident.6.3m/s
Test 4	983s	6.5285m/s	Valid.6.3m/s

Table 2.: Measurement time series from the real wind turbine

As can be seen from the Table 2, Test 1 and 2 have the same mean wind speed. Hence, Test 1 data can be used for model identification, while Test 2 can be used as validation data at 4.5m/s. The same hold for Test 3 and 4, where mean wind speed is 6.3m/s.

3.1.2 Tower First fore-aft mode identification

In order to estimate the tower first fore aft modal frequency and damping, the transfer function from pitch angle demand θ to the tower top fore-aft velocity v_{nod},.is identified. For identification the test set Test 1 and test 3 are used.
Figure 4 compare the bode plots of the identified models at 4.5m/s with the linearized model (indicated as Lin. mod.) at 5m/s.
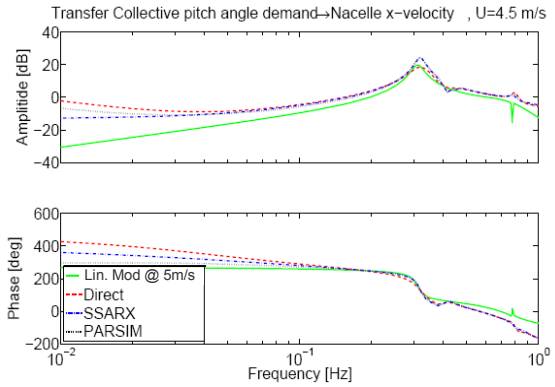

Figure 4.: Bode plot of the identified tower fore-aft models at mean wind speed of 4.5m/s and linearized model at 5m/s

From Figure 4, it can be observed that the identified models are very well comparable to the l models around the first tower frequency.

Given the identified models, the corresponding frequency and damping are computed as explained in section 2.1.4.

The modal frequencies and logarithmic decrements, computed from the identified modes are compared to those obtained from the linearized models at 5 and 7m/s.

Wind [m/s]	Method	Freq [Hz]	Log.decr [%]
5	Lin. Mod.	0.3133	27.45
4.5	Direct	0.3195	36.8
4.5	SSARX	0.3202	27.41
4.5	PARSIM	0.3204	21.38
7	Lin. mod.	0.3161	33.49
6.3	Direct	0.3228	35.05
6.3	SSARX	0.3222	36.85
6.3	PARSIM	0.3278	29.55

Table 3.: Frequency and logarithmic decrement of the tower first fore-aft mode

The validation results, based on sets Test 2 and Test 4, are summarized in the following table.

Wind [m/s]	Method	VAF	PEC (x10^{-5})	R_{ix}^{ε}	$R_{ix}^{\varepsilon u}$ (x10^{-2})
4.5	Direct	97.43	3.592	0.7129	1.2
4.5	SSARX	97.26	3.706	2.744	1.344
4.5	PARSIM	95.99	4.487	2.517	6.346
6.3	Direct	97.36	4.684	0.7638	3.59
6.3	SSARX	97.36	4.68	0.6674	3.843
6.3	PARSIM	97.18	4.841	0.8528	4.164

Table 4.: Validation results for identified models of the tower first fore aft.

As can be seen from Table 4, the validation results indicate that all models have comparable high accuracy.

3.1.3 Tower First side to side mode identification

Similarly, to estimate the tower first side to side modal frequency and damping, the transfer function from generator torque demand T_g to the tower top side to side velocity v_{nay} is identified.
Next figure shows the comparison of the bode plots of the identified models at 6.3m/s with linearized model at 7m/s.
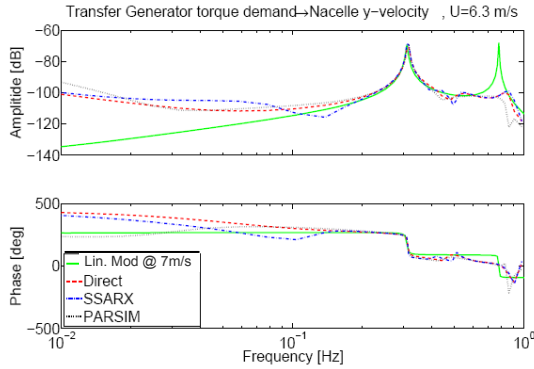

Figure 5.: Bode plot of the identified tower side to side models at mean wind speed of 6.3m/s

It can be observed the good overlap between the identified models and the linearized model. Those similarities are quantified in terms of frequency and logarithmic decrement in the following table.

Wind [m/s]	Method	Freq [Hz]	Log.decr [%]
5	Lin. mod.	0.3115	5.426
4.5	Direct	0.3151	3.037
4.5	SSARX	0.3156	2.549
4.5	PARSIM	0.3147	4.763
7	Lin. mod.	0.3115	5.556
6.3	Direct	0.3148	5.883
6.3	SSARX	0.3143	2.17
6.3	PARSIM	0.3153	3.861

Table 5.: Frequency and logarithmic decrement of the tower first sidewards mode

The time domain validation results are shown in Table 6.

Wind [m/s]	Method	VAF	PEC (x10^{-5})	R_{ix}^{ε}	$R_{ix}^{\varepsilon u}$
4.5	Direct	99.99	4.487	1.118	8.9x10^{-3}
4.5	SSARX	99.99	4.506	1.174	0
4.5	PARSIM	99.99	4.03	1.467	0.136
6.3	Direct	99.99	5.514	0.8991	0
6.3	SSARX	99.99	5.399	0.8085	0
6.3	PARSIM	99.99	6.557	0.9674	0.1165

Table 6.: Validation results for identified models of the tower first sidewards mode

3.1.4 First drive train mode

Finally, the first drive train frequency and damping are estimated from the identified transfer function from the generator torque demand T_g to the generator speed Ω.
Next figure shows the Bode plots of the transfer functions identified with the Direct, SSARX and PARSIM method, compared to the linear model obtained from the aerolastic code.
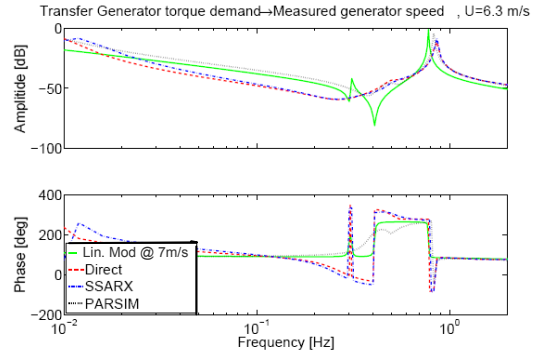

Figure 6.: Bode plot of the identified first drive train models at mean wind speed of 6.3m/s

As can be observed in the figure above, the identified drive-train frequency is about 10% higher than the linearized model.

Wind [m/s]	Method	Freq [Hz]	Log.decr [%]
5	Lin. mod.	0.7777	1.304
4.5	Direct	0.8773	14.12
4.5	SSARX	0.878	16.61
4.5	PARSIM	0.8261	6.877
7	Lin. mod.	0.778	1.642
6.3	Direct	0.8496	1.499
6.3	SSARX	0.8534	1.822
6.3	PARSIM	0.8305	3.857

Table 7.: Frequency and logarithmic decrement of the first drive train mode.

Comparing the linearized model obtained with the aerolastic code with the identified model using PARSIM method, better estimation is obtained. In any case, the drive train frequency is not well present in the input-output data.
In contrast with the frequency domain results showed in Table 7, the Time domain validation methods shows excellent results.

Wind [m/s]	Method	VAF	PEC (x10^{-3})	R_{ix}^{ε}	$R_{ix}^{\varepsilon u}$
4.5	Direct	99.98	6.797	0.0707	0.7321
4.5	SSARX	99.98	6.731	0.0508	0.6704
4.5	PARSIM	99.96	10.04	0.8471	0.856
6.3	Direct	100	5.97	0.24	0.0996
6.3	SSARX	100	5.962	0.181	0.2558
6.3	PARSIM	100	6.908	0.13	0.4208

Table 8.: Validation results for identified models of the first drive train mode
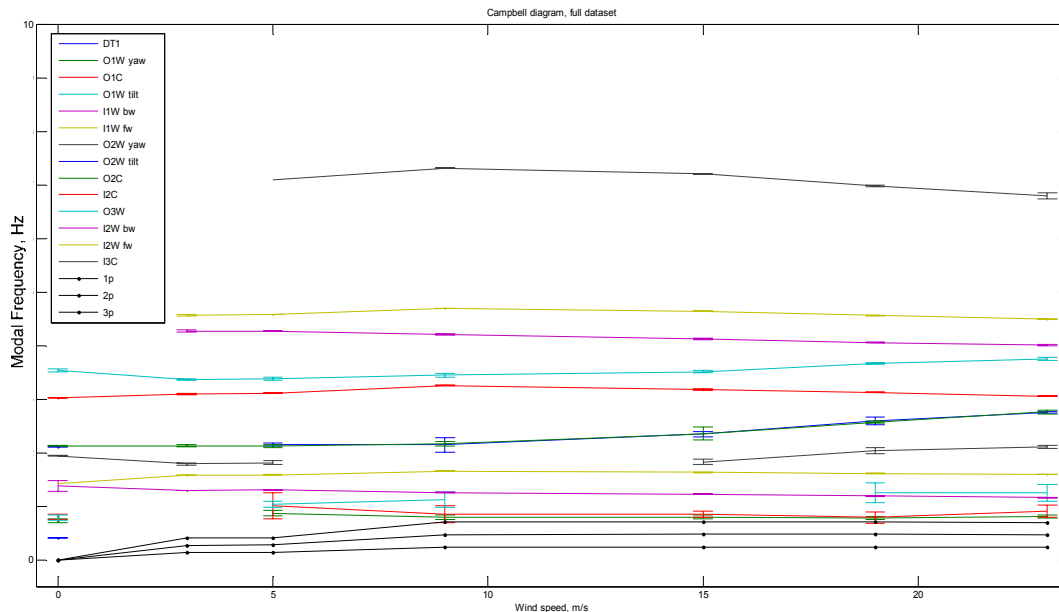
Figure 7.: Modal frequency as a function of wind speed. Letters in the mode name: "O" – out-of-plane, "I" – inplane, "C" -- collective, "W" – whirling; "bw" – backward; "fw" – forward; "DT" – drive-train mode; 1p, 2p, 3p – fundamental frequency and its first two harmonics.

A justification for those differences could be either that the drive-train frequency is not well represented in the data due to the presence of a drive-train damping filter existing in the control or that in reality, the drive train is less flexible than in the lineraized model obtained from the aerolastic code.

Further experiments needs to be performed to clarify the exact reason of this divergence.

3.2 Operational Modal Analysis Results

In order to ensure feasibility of the application of OMA to operational wind turbine, a series of numerical experiments were conducted. Using commercial aeroelastic software, the acceleration time histories for the following locations were synthesized:

- points on the different blade radii;

- hub;

- points on the different heights of the tower.

The data was accompanied with the time histories for azimuth and pitch angles, rotor RPM, wind speed and direction, etc.

The acceleration data from the blades were subjected to Coleman transformation and then used as the input to commercial OMA software, where the modal parameters were extracted. Figure 7 presents the obtained modal frequency for the rotor-related modes as a function of the wind speed (Campbell diagram). Note, sometimes it was not possible to extract some of the modes for specific wind speeds. Confidence intervals (shown as vertical line segments) were found to be a useful tool for judging applicability of OMA to specific operational conditions (wind speed/pitch/rotor RPM). Figure 8 shows the Campbell diagram for modal damping (in-plane and out-of-plane rotor-related modes). Similar graphs were obtained for the damping, and for modal parameters of the tower-related modes.

Using backward Coleman transformation, mode shapes were calculated and visualized (Figure 9); this visualization played an important role in mode identification.

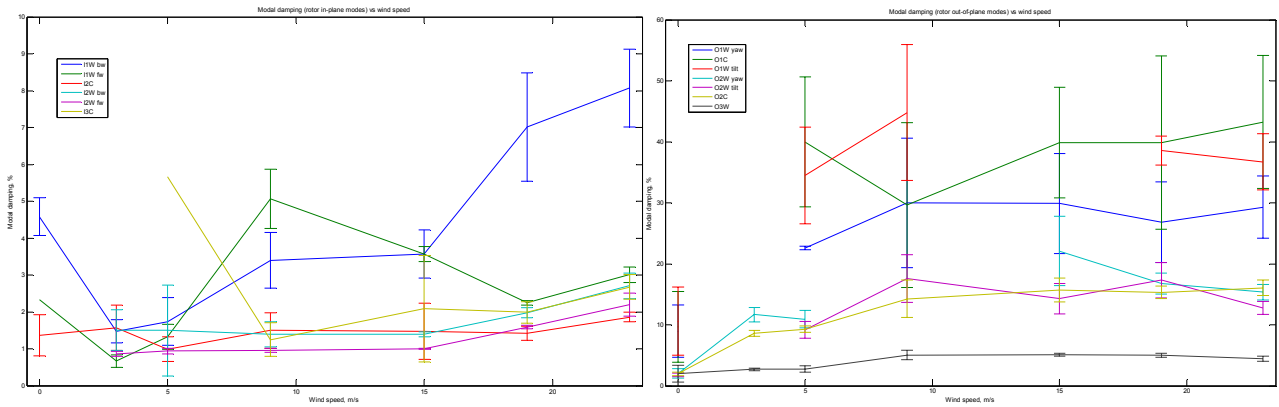Work is currently ongoing to apply OMA on a real wind turbine.

Figure 8. Modal damping as a function of wind speed. Top: in-plane modes; Bottom: out-of-plane modes
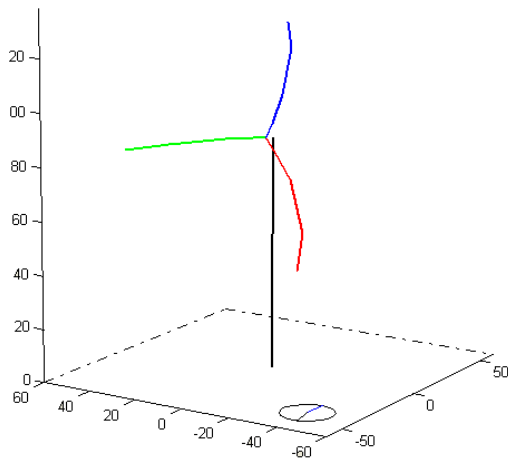

Figure 9.: Visualization of mode shape

4 Conclusions

Theory and results of two different system identification methods for estimating modal parameters of a wind turbine in operation have been presented.

In the first method, additional excitation on the controllable inputs of the turbine (pitch and/or generator) is needed. These signals are designed in such a way that accurate models are identified and no unacceptable turbine loads occur. In order to validate the identified open-loop models, both time-domain validation methods and frequency-domain comparisons to linearized aeroelastic models are made. The results show good match in frequency and damping ratio for a frequency range up to 1Hz. The time domain validation indexes indicate in all cases good model quality. Although no

frequency-domain validation is possible due to the lack of information about the all excitation signals, Frequency domain comparison can be performed using linearized models at mean wind speeds of 5 and 7m/s. This comparison shows very good overlap around the first tower fore-aft and side to side frequencies, but some discrepancies are found at first drive train frequencies. Further experiments need to be performed to clarify the exact reason of this divergence by either increasing the generator torque excitation amplitude or by de-activating the drive-train filter in the controller.

In the second method, only output measurements were used. A feasibility study has been performed on simulation data in order to investigate the possibility of using OMA to identify the dynamic characteristics of a wind turbine under operation. OMA techniques are applied using time domain response data obtained from simulations carried out with an aeroelastic code. Response data is obtained at the locations coinciding (or located close to) future real wind turbine measurement locations. Results presented as Campbell diagrams show promising applicability of OMA techniques in an operating wind turbine.

Major differences between both methods are mainly the frequency range that can be identified, the equipment needed for implementation and the modal information extracted. The use of PRBS methods, allows extracting the transfer functions directly, which are used in control design. However, limitations on the actuators bound the identification frequency range.

On the other side, OMA techniques allow to extract the mode shapes. However, dedicated equipment is needed to extract the relevant data.

At last, using those methods, the modal parameters estimated can be used for either improving the existing control loops, for achieving additional functionality by designing new control strategies for fatigue reduction or for updating the existing FEM and multibody models.

References

[1] Bialasiewicz, J. (1995): *Advanced System Identification Techniques for Wind Turbine Structures*. Report NREL/TP-442-6930, NREL. Prepared for the 1995 SEM Spring Conference, Grand Rapids, Michigan, USA.

[2] Marrant, B. and T. van Holten (2004): System Identification for the analysis of aeroelastic stability of wind turbine blades. Proceedings of the European Wind Conference & Exhibition, pp. 101--105.
http://www.2004ewec.info/files/23_1400_benjaminmarrant_01.pdf

[3] Hansen, M.H., K. Thomsen, P. Fuglsang and T. Knudsen (2006): Two methods for estimating aeroelastic damping of operational wind turbine modes from experiments. Wind Energy, 9(1--2):179--191.

[4] Novak, P., T. Ekelund, I. Jovik and B. Schmidtbauer (1995): Modeling and control of variable-speed wind-turbine drive-system dynamics. IEEE Control Systems, 15(4):28--38.

[5] Ljung, L. (1999): System Identification. Theory for the User. Prentice Hall.

[6] van den Hof, P. and X. Bombois (2004): System Identification for Control. Delft Center for Systems and Control, TU-Delft. Lecture notes, Dutch Institute for Systems and Control (DISC)

[7] van den Hof, P. and M. Gilson (2001): Closed-loop system identification via a tailor-made IV method. Proceedings of the 40th Conference on Decision and Control. Orlando, Florida, pp. 4314--4319.
www.dcsc.tudelft.nl/~pvandenhof/Paperfiles/GilsonVdHof-CDC2001.PDF

[8] Van Overschee, P. and B. De Moor (1997): Closed-loop Subspace System Identification. Proceedings of the 36th Conference on Decision and Control. San Diago, California, USA.

[9] Qin, S. and L. Ljung (2003): Closed-Loop Subspace Identification with Innovation Estimation. Proceedings of the 13th IFAC Symposium on System Identification, pp. 887--892.

[10] Ljung, L. and T. McKelvey (1996): Subspace identification from closed loop data. Signal Processing, 52:209--215.

[11] S. Chauhan, M.H. Hansen, D. Tcherniak (2009), Application of Operational Modal Analysis and Blind Source Separation / Independent Component Analysis Techniques to Wind Turbines, Proceedings of XXVII International Modal Analysis Conference, Orlando (FL), USA, Feb. 2009

[12] D. Tcherniak, S. Chauhan, M. Rosseti, I. Font, J. Basurko, O. Salgado (2010), *Output-only Modal Analysis on Operating Wind Turbines: Application to Simulated Data, to appear in Proceedings of European Wind Energy Conference, Warsaw, Poland, Apr. 2010.*

[13] D. Tcherniak, S. Chauhan, M.H. Hansen (2010), *Applicability Limits of Operational Modal Analysis to Operational Wind Turbines, Proceedings of XXVIII International Modal Analysis Conference, Jacksonville (FL), USA, Feb. 2010*